



## COVER SHEET

---

**This is the author version of an article published as:**

**Frost, Ray L. and Bouzaid, Jocelyne M. (2007) Raman spectroscopy of dawsonite  $\text{NaAl}(\text{CO}_3)(\text{OH})_2$ . *Journal of Raman Spectroscopy* 38(7):pp. 873-879.**

**Copyright 2007 John Wiley & Sons**

**Accessed from <http://eprints.qut.edu.au>**

## Raman spectroscopy of dawsonite $\text{NaAl}(\text{CO}_3)(\text{OH})_2$

Ray L. Frost\* and Jocelyn M. Bouzaid

Inorganic Materials Research Program, School of Physical and Chemical Sciences, Queensland University of Technology, GPO Box 2434, Brisbane Queensland 4001, Australia.

### Abstract

Raman spectroscopy at both 298 and 77 K complimented with infrared spectroscopy has been used to study the structure of dawsonite. Previous crystallographic studies concluded that the structure of dawsonite was a simple one, however both Raman and infrared spectroscopy show that this conclusion is incorrect. Multiple bands are observed in both the Raman and infrared spectra in the antisymmetric stretching and bending regions showing that the symmetry of the carbonate anion is reduced and in all probability the carbonate anions are not equivalent in the dawsonite structure. Multiple OH deformation vibrations centred upon  $950\text{ cm}^{-1}$  in both the Raman and infrared spectra show that the OH units in the dawsonite structure are non-equivalent. Calculations using the position of the Raman and infrared OH stretching vibrations enabled estimates of the hydrogen bond distances of 0.2735, 0.27219 pm at 298 K and 0.27315, 0.2713 pm at 77 K to be made. This indicates strong hydrogen bonding of the OH units in the dawsonite structure.

**Key words:** barentsite, dawsonite, tunisite, smithsonite, carbonate, hydroxyl, Infrared and Raman spectroscopy

### Introduction

Dawsonite, a sodium aluminium hydroxy carbonate  $\text{NaAl}(\text{CO}_3)(\text{OH})_2$ , is orthorhombic with point group  $2/m$ <sup>1</sup> and is acicular to bladed crystals and often occurs in rosettes and radial fibrous to tufted aggregates<sup>2</sup>. The mineral is formed through low temperature hydrothermal decomposition of aluminous silicates<sup>3,4</sup>. Varieties other than sodium dawsonite are known<sup>5-7</sup>. Indeed dawsonites with yttrium and cerium are also known<sup>8,9</sup>. Many of these types of synthetic compounds are used as catalyst precursors<sup>10-13</sup>. Dawsonite formation is used in water purification for the removal of alumina species<sup>14</sup>. It is possible that this type of mineral can be used to trap carbon dioxide and remove green house gases. A model of the mineral is given in Figure 1. Rotation of the figure shows that the mineral contains a hole in the structure which makes the mineral take on a zeolite type structure. It is possible that this space might be used to trap heavy metals.

The infrared spectra of dawsonite has been published<sup>15-21</sup>. Alumina surfaces have been analysed by FTIR spectroscopy<sup>18</sup>. Some reports of the Raman spectra have been published<sup>16,19</sup>. The free ion,  $\text{CO}_3^{2-}$  with  $D_{3h}$  symmetry exhibits four normal vibrational modes; a symmetric stretching vibration ( $\nu_1$ ), an out-of-plane bend ( $\nu_2$ ), a

---

\* Author to whom correspondence should be addressed (r.frost@qut.edu.au)

doubly degenerate asymmetric stretch ( $\nu_3$ ) and another doubly degenerate bending mode ( $\nu_4$ )<sup>22-25</sup>. The symmetries of these modes are  $A_1'$  (R) +  $A_2''$  (IR) +  $E'$  (R, IR) +  $E''$  (R, IR) and occur at 1063, 879, 1415 and 680  $\text{cm}^{-1}$  respectively. Generally, strong Raman modes appear around 1100  $\text{cm}^{-1}$  due to the symmetric stretching vibration ( $\nu_1$ ), of the carbonate groups, while intense IR and weak Raman peaks near 1400  $\text{cm}^{-1}$  are due to the antisymmetric stretch ( $\nu_3$ ). Infrared modes near 800  $\text{cm}^{-1}$  are derived from the out-of-plane bend ( $\nu_2$ ). Infrared and Raman modes around 700  $\text{cm}^{-1}$  region are due to the in-plane bending mode ( $\nu_4$ ). This mode is doubly degenerate for undistorted  $\text{CO}_3^{2-}$  groups. As the carbonate groups become distorted from regular planar symmetry, this mode splits into two components. Infrared and Raman spectroscopy provide sensitive test for structural distortion of  $\text{CO}_3^{2-}$ .

To date little Raman spectra of dawsonite has been published, even though a significant number of infrared analyses have been undertaken<sup>15,17-21</sup>. X-ray crystallography suggests the mineral has a regular structure. However the infrared data suggests otherwise.

## Experimental

### *Minerals*

Selected dawsonite minerals were obtained from the Mineral Research Company (<http://www.minresco.com/default.htm>) and other sources including Museum Victoria (Museum Victoria, Melbourne, Victoria, Australia). The samples were phase analysed by powder X-ray diffraction and for chemical composition by EDX measurements.

### *Raman microprobe spectroscopy*

The crystals of dawsonite were placed and oriented on the stage of an Olympus BHSM microscope, equipped with 10x and 50x objectives and part of a Renishaw 1000 Raman microscope system, which also includes a monochromator, a filter system and a Charge Coupled Device (CCD). Raman spectra were excited by a HeNe laser (633 nm) at a resolution of 3.5  $\text{cm}^{-1}$  in the range between 100 and 4000  $\text{cm}^{-1}$ . Repeated acquisition using the highest magnification was accumulated to improve the signal to noise ratio.

Spectra were calibrated using the 520.5  $\text{cm}^{-1}$  line of a silicon wafer. Previous studies by the authors provide more details of the experimental technique. Spectra at liquid nitrogen temperature were obtained using a Linkam thermal stage (Scientific Instruments Ltd, Waterfield, Surrey, England). Details of the technique have been published by the authors<sup>26-29</sup>.

### *Mid-IR spectroscopy*

Infrared spectra were obtained using a Nicolet Nexus 870 FTIR spectrometer with a smart endurance single bounce diamond ATR cell. Spectra over the 4000–525  $\text{cm}^{-1}$  range were obtained by the co-addition of 64 scans with a resolution of 4  $\text{cm}^{-1}$

and a mirror velocity of 0.6329 cm/s. Spectra were co-added to improve the signal to noise ratio.

Spectral manipulation such as baseline adjustment, smoothing and normalisation were performed using the Spectracalc software package GRAMS (Galactic Industries Corporation, NH, USA).

Band component analysis was undertaken using the Jandel 'Peakfit' software package which enabled the type of fitting function to be selected and allows specific parameters to be fixed or varied accordingly. Band fitting was done using a Lorentz-Gauss cross-product function with the minimum number of component bands used for the fitting process. The Lorentz -Gauss ratio was maintained at values greater than 0.7 and fitting was undertaken until reproducible results were obtained with squared correlations of  $r^2$  greater than 0.9995.

## Results and discussion

The Raman spectra of dawsonite at 298 and 77 K are shown in Figures 2a and 2b. The infrared spectrum of the two selected dawsonites are shown in Figure 3. The spectral region centred upon  $1090\text{ cm}^{-1}$  is complex with a number of overlapping bands. Two distinct bands are observed in the 298 K spectra at  $1090$  and  $1065\text{ cm}^{-1}$  for the dawsonite from Italy and  $1090$  and  $1066\text{ cm}^{-1}$  for the dawsonite from Canada. These bands are attributed to the  $\nu_1$  symmetric stretching modes. According to Farmer<sup>30</sup> the structure of dawsonite is stated to be quite regular. The structural analysis of dawsonite suggests that the  $(\text{CO}_3)^{2-}$  ion is regular and is not involved with bonding<sup>3,4,31</sup>. This suggestion is not consistent with the Raman spectrum as multiple bands are observed in the  $(\text{CO}_3)^{2-}$  stretching region. This observation is even more pronounced upon obtaining the Raman spectra at 77 K. Three resolvable bands are observed at  $1103$ ,  $1091$  and  $1070\text{ cm}^{-1}$  for the dawsonite from Italy and at  $1103$ ,  $1091$  and  $1070\text{ cm}^{-1}$  for the dawsonite from Canada. Farmer also reported the  $\nu_1$  band to be two quite distinct bands unusual for a single  $(\text{CO}_3)^{2-}$  ion<sup>30</sup>. Fundamentally there is no difference between the spectra of the two mineral samples. Any differences are very small.

A very low intensity band is observed in both spectra at  $1367\text{ cm}^{-1}$ . In the infrared spectra of dawsonite (this work) an intense asymmetric band is observed at  $1390\text{ cm}^{-1}$  (Figure 3). Component bands may be resolved as is shown in this figure. This value is in excellent agreement with previously published data<sup>30,32</sup>. Two Raman bands are also observed in the 298 K spectra at  $1505$  and  $1483\text{ cm}^{-1}$ . In the infrared spectra an asymmetric band at  $1542\text{ cm}^{-1}$  is observed with band components resolved at  $1588$ ,  $1542$ ,  $1489\text{ cm}^{-1}$ . These spectra confirm the assertion that the spectra of dawsonite is not simple but shows complexity in each spectral region. The observation of multiple bands in the antisymmetric stretching region is an indication of the reduction in symmetry of the carbonate ion in the dawsonite structure. An alternative explanation is that in the structure not all the carbonates are identical as is observed in Figure 1. These bands at  $1505$  and  $1483$  are attributed to the  $\nu_3$  antisymmetric stretching mode. Estep and Karr assigned an infrared band at  $1550\text{ cm}^{-1}$  to the OH bending mode and the band at  $1390\text{ cm}^{-1}$  to the antisymmetric stretching mode<sup>15</sup>. The fact that multiple bands may be resolved in the infrared spectra suggest that the infrared bands as described by Frueh and Golightly is an over

simplification. They assigned both the high wavenumber bands to the  $\nu_3$  antisymmetric stretching mode<sup>32</sup>. The normal average band position of the  $\nu_3$  antisymmetric stretching mode is around  $1470\text{ cm}^{-1}$ . Farmer, based upon infrared spectroscopy of Frueh and Golightly, reported two antisymmetric stretching modes at  $1550$  and  $1390\text{ cm}^{-1}$ <sup>30</sup>. Upon the collection of Raman spectral data at  $77\text{ K}$ , bands are observed at  $1505$ ,  $1484$  and  $1367\text{ cm}^{-1}$ . The last band is of very low intensity in the Raman spectra and is only observed through scale expansion.

In the infrared spectrum of dawsonite as reported by Frueh and Golightly, bands were observed at  $858$  and  $842\text{ cm}^{-1}$  and were attributed to the  $\nu_2$  bending mode of the carbonate anion<sup>32</sup>. In the Raman spectrum of dawsonite from Italy a band is observed at  $822\text{ cm}^{-1}$  assigned to the  $\nu_2$  bending mode (Figure 4a). The infrared spectra of the two dawsonites are shown in Figure 5. A quite low intensity band is observed for dawsonite from Canada at  $826\text{ cm}^{-1}$ . Multiple bands are observed in the infrared spectra around  $845\text{ cm}^{-1}$ . Bands are observed at  $883$ ,  $863$ ,  $845$  and  $841\text{ cm}^{-1}$  for the dawsonite from Italy. Bands in an almost identical position are observed for the dawsonite from Canada.

Two bands are observed in the Raman spectra for both dawsonite samples at  $934$  and  $897\text{ cm}^{-1}$ . In the infrared spectrum (Figure 5) multiple bands are observed at around  $950\text{ cm}^{-1}$  with component bands at  $953$ ,  $934$  and  $920\text{ cm}^{-1}$ . For the dawsonite from Italy the latter band is higher in intensity and for the dawsonite from Canada the former band is of higher intensity. This indicates an orientation effect on the Raman spectra of dawsonite. Frueh and Golightly reported two infrared bands at  $950$  and  $930\text{ cm}^{-1}$  and Farmer assigned these bands to OH deformation modes. Thus the two Raman bands at  $934$  and  $897\text{ cm}^{-1}$  are attributed to the OH deformation bands of dawsonite. These bands show significant shifts to higher wavenumbers upon cooling to  $77\text{ K}$  (Figure 4b). The bands are observed at  $948$  and  $902\text{ cm}^{-1}$ . This is a  $14$  and  $7\text{ cm}^{-1}$  shift. Such a shift is not observed for the other low wavenumber bands and supports the concept that these bands are assignable to OH deformation modes. The observation of multiple bands proves that all the OH units are not equivalent. In the X-ray crystallographic structure of dawsonite all OH units are defined as equivalent. Both Raman and infrared spectroscopy suggests this is not correct.

At  $77\text{ K}$  only one band is observed at  $826\text{ cm}^{-1}$  assigned to the  $\nu_2$  bending mode of carbonate anion. In the Raman spectra of the low wavenumber region two bands are observed for both the dawsonite mineral samples at  $746$  and  $729\text{ cm}^{-1}$ . Frueh and Golightly reported only one band at  $727\text{ cm}^{-1}$  in the infrared spectrum of dawsonite. The band is attributed to the  $\nu_4$  bending mode. In the infrared spectrum of dawsonite from Italy bands are observed at  $730$ ,  $696$  and  $670\text{ cm}^{-1}$  and are assigned to the  $\nu_4$  bending mode. The infrared spectrum of the dawsonite from Canada is identical with bands in the same positions. The observation of multiple bands in the  $\nu_4$  region provides further evidence for the nonequivalence of the carbonate units in the dawsonite structure.

In the region below  $700\text{ cm}^{-1}$  a significant number of Raman bands are observed. An intense band at  $587\text{ cm}^{-1}$  observed in the  $298\text{ K}$  spectrum (Figure 4a) and at  $592\text{ cm}^{-1}$  in the  $77\text{ K}$  spectrum (Figure 4b) is assigned to an AlO stretching vibration. Frueh and Golightly reported a band at  $685\text{ cm}^{-1}$  and assigned the band to

this vibrational mode<sup>32</sup>. Serna et al. attributed most of the vibrational bands below 700 cm<sup>-1</sup> to AIO modes<sup>19</sup>. It is probable that the band at 519 cm<sup>-1</sup> is also attributable to an AIO symmetric stretching vibration. Two bands are observed at ~386 and 360 cm<sup>-1</sup> and may be assigned to OAlO bending modes. A number of Raman bands are observed at 260, 218, 189 and 150 cm<sup>-1</sup>. Significant band narrowing is observed for these bands upon obtaining the Raman spectra at 77 K.

The Raman spectra of the OH stretching region at 298 and 77 K are shown in Figures 6a and 6b. The infrared spectra of the two dawsonites in the OH stretching region are shown in Figure 7. A complex set of bands with an overlapping profile is observed. Two bands are found at 298 K for the dawsonites at 3282 and 3250 cm<sup>-1</sup>. There is a distinct shift to lower wavenumbers upon cooling to 77 K where bands at 3274 and 3227 cm<sup>-1</sup> are observed. In the infrared spectrum two component bands at 3275 and 3244 cm<sup>-1</sup> are observed with additional low intensity bands at 3461 and 3364 cm<sup>-1</sup>. The infrared spectrum of dawsonite is strongly asymmetric on the low wavenumber side and component bands are resolved as shown in Figure 7. These bands may be attributed to adsorbed water. Studies have shown a strong correlation between OH stretching frequencies and both O···O bond distances and H···O hydrogen bond distances<sup>33-36</sup>. Libowitzky (1999) showed that a regression function can be employed relating the hydroxyl stretching frequencies with regression coefficients better than 0.96 using infrared spectroscopy<sup>37</sup>. The function is described as:  $\nu_1 = (3592 - 304) \times 109^{\frac{-d(O-O)}{0.1321}} \text{ cm}^{-1}$ . Thus OH---O hydrogen bond distances may be calculated using the Libowitzky empirical function. The values for the OH stretching vibrations listed above provide hydrogen bond distances of 0.2735 pm (3282 cm<sup>-1</sup>), 0.27219 pm (3250 cm<sup>-1</sup>) for the 298 K spectra and 0.27315 pm (3274 cm<sup>-1</sup>), 0.2713 pm (3227 cm<sup>-1</sup>) for the 77 K spectra. Frueh and Golightly suggested some hydrogen bonding exists for dawsonite<sup>32</sup>. The values calculated here support the concept of strong hydrogen bonding between the OH units and the carbonate anions in the dawsonite structure.

## Conclusions

This study has shown the structure of dawsonite is not a simple structure as is evidenced from X-ray crystallography. Multiple bands are observed in both the Raman and infrared spectra in the carbonate stretching and bending modes indicating a symmetry reduction of the carbonate anion. An alternative explanation for the observation of multiple bands is the nonequivalence of the carbonate anions in the dawsonite structure. Multiple bands attributed to the OH deformation modes support the concept of nonequivalent OH units in the dawsonite structure. Calculations based on a Libowitzky type expression enabled estimates of the hydrogen bond distances between the OH units in dawsonite and the carbonate anions to be made. Hydrogen bond distances of 0.2735 and 0.27219 pm show strong hydrogen bonding.

## Acknowledgments

The financial and infra-structure support of the Queensland University of Technology, Inorganic Materials Research Program is gratefully acknowledged. The Australian Research Council (ARC) is thanked for funding the instrumentation. Mr

D. A. Henry of Museum Victoria (Melbourne, Australia) is thanked for the loan of the dawsonite mineral samples.

## References

1. Corazza, E, Sabelli, C, Vannucci, S. *Neues Jahr. Mineral.* 1977: 381.
2. Anthony, JW, Bideaux, RA, Bladh, KW, Nichols, MC *Handbook of Mineralogy*; Mineral Data Publishing: Tiscan, Arizona, USA, 2003; Vol. 5.
3. Smirnov, MN, Bitner, AA, Tsekhovolskaya, DI, Nikolaeva, LY. *Nov. Nebok.* 1982: 228.
4. Kwon, SW. *Taehan Hwahakhoe Chi* 1969; **13**: 157.
5. Dunning, GE, Henderson, WA, Jr. *Riv. Mineral. Ital.* 2003: 102.
6. Iga, T, Kato, S. *Yogyo Kyokaishi* 1978; **86**: 509.
7. Zhang, X, Wen, Z, Gu, Z, Xu, X, Lin, Z. *J. Solid State Chem.* 2004; **177**: 849.
8. Grice, JD, Gault, RA. *Can. Min.* 2006; **44**: 105.
9. Grice, JD, Gault, RA, Roberts, AC, Cooper, MA. *Can. Min.t* 2000; **38**: 1457.
10. Kwon, SW, Kim, BH, Ishikawa, H. *Kogyo Kagaku Zasshi* 1971; **74**: 1992.
11. Kwon, SW, Kim, BH, Ishikawa, H. *Kogyo Kagaku Zasshi* 1971; **74**: 1987.
12. Li, J-G, Ikegami, T, Lee, J-H, Mori, T, Yajima, Y. *J. Euro. Ceram. Soc.* 2001; **21**: 139.
13. Ali, AA, Hasan, MA, Zaki, MI. *Chem. Mater.* 2005; **17**: 6797.
14. Alvarez-Ayuso, E, Nugteren, HW. *Water Res.* 2005; **39**: 2096.
15. Estep, PA, Karr, C, Jr. *Am. Miner.* 1968; **53**: 305.
16. Garcia-Ramos, JV, Serna, CJ. *Rev. Acad. de Cien.* 1987; **81**: 397.
17. Karr, C, Jr., Kovach, JJ. *App. Spec.* 1969; **23**: 219.
18. Lee, DH, Condrate Sr, RA. *Mat. Let.* 1995; **23**: 241.
19. Serna, CJ, Garcia-Ramos, JV, Pena, MJ. *Spect. Acta*, 1985; **41A**: 697.
20. Su, C, Suarez, DL. *Clays Clay Miner.* 1997; **45**: 814.
21. Tsekhovolskaya, DI, Nikolaeva, LY. *Nov. Neboksit. Vidy Glinozem. Syr'ya, M.* 1982: 231.
22. Frost, RL, Weier, ML, Cejka, J, Ayoko, GA. *Spectrochim. Acta*, 2006; **65**: 529.
23. Frost, RL, Erickson, KL, Weier, ML, Carmody, O, Cejka, J. *J. Mol. Struct.* 2005; **737**: 173.
24. Frost, RL, Williams, PA, Martens, W. *Min. Mag.* 2003; **67**: 103.
25. Frost, RL, Martens, WN, Rintoul, L, Mahmutagic, E, Kloprogge, JT. *J. of Ram. Spec.* 2002; **33**: 252.
26. Frost, RL, Henry, DA, Erickson, K. *J. of Ram. Spec.* 2004; **35**: 255.
27. Frost, RL. *Spectrochim. Act.*, y 2004; **60A**: 1469.
28. Frost, RL, Carmody, O, Erickson, KL, Weier, ML, Cejka, J. *J. Mol. Struct.* 2004; **703**: 47.
29. Frost, RL, Carmody, O, Erickson, KL, Weier, ML, Henry, DO, Cejka, J. *J. Mol. Struct* 2004; **733**: 203.
30. Farmer, VC *Mineralogical Society Monograph 4: The Infrared Spectra of Minerals*, 1974.
31. Mandarino, JA, Harris, DC. *Can. Min.* 1965; **8**: 377.
32. Frueh, AJ, Jr., Golightly, JP. *Can. Min.* 1967; **9**: 51.
33. Emsley, J. *Chem. Soc. Rev.* 1980; **9**: 91.
34. Lutz, H. *Structure and Bonding (Berlin, Germany)* 1995; **82**: 85.
35. Mikenda, W. *J. Mol. Struct.* 1986; **147**: 1.
36. Novak, A. *Struct. Bond.* 1974; **18**: 177.
37. Libowitzky, E. *Monat.e für chem.* 1999; **130**: 1047.





*List of Figures*

**Figure 1 Molecular model of dawsonite**

**Figure 2a and 2b Raman spectra of dawsonite in the 1000 to 2000  $\text{cm}^{-1}$  range at 298 and 77 K.**

**Figure 3 Infrared spectra of dawsonite in the 1200 to 1800  $\text{cm}^{-1}$  range**

**Figure 4a and 4b Raman spectra of dawsonite in the 100 to 1000  $\text{cm}^{-1}$  range at 298 and 77 K.**

**Figure 5 Infrared spectra of dawsonite in the 500 to 1200  $\text{cm}^{-1}$  range**

**Figure 6a and 6b Raman spectra of dawsonite in the 3100 to 3500  $\text{cm}^{-1}$  range at 298 and 77 K.**

**Figure 7 Infrared spectra of dawsonite in the 2700 to 3700  $\text{cm}^{-1}$  range**

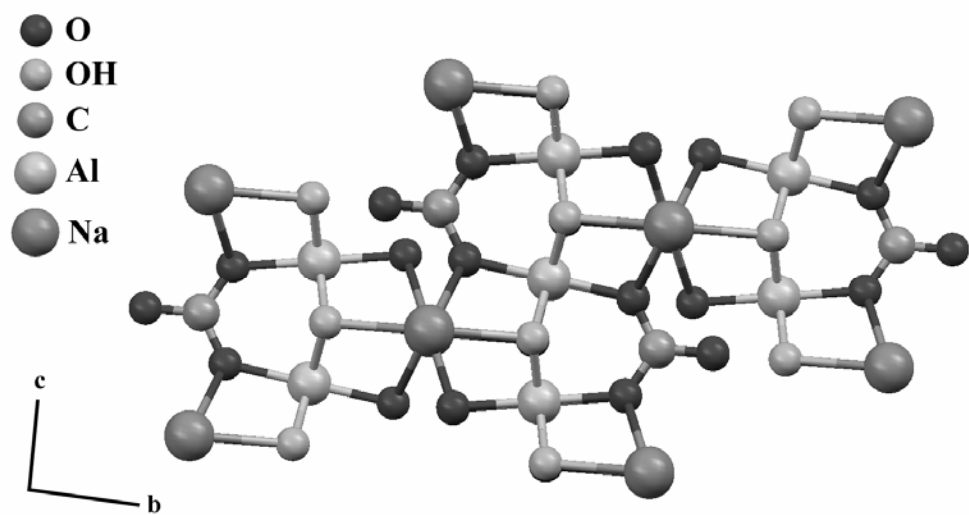


**Figure 1**

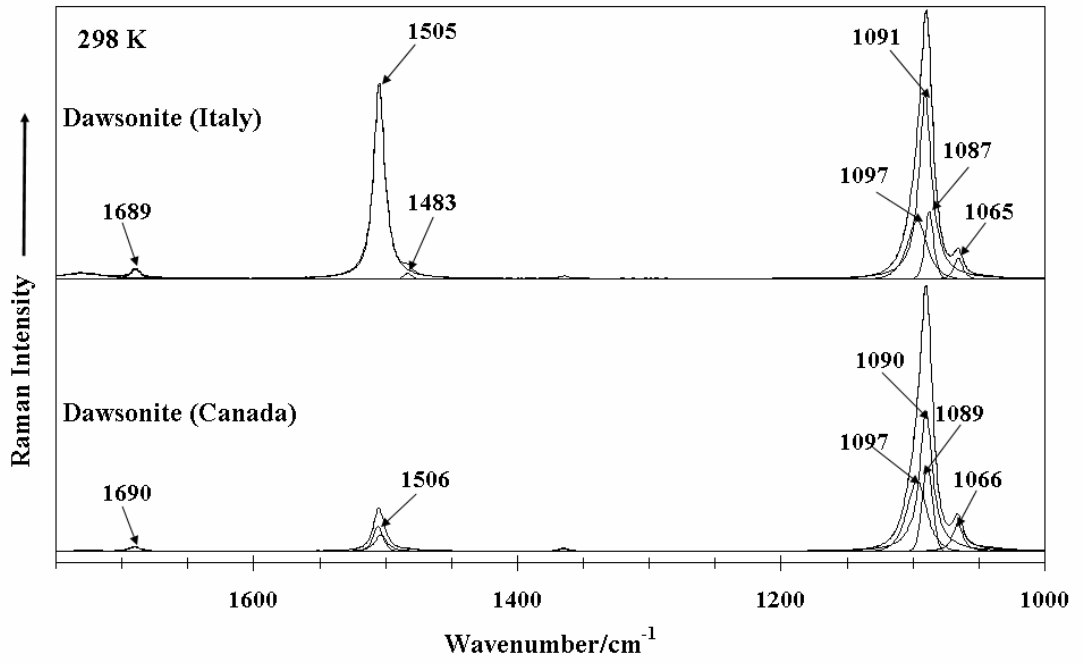


Figure 2a

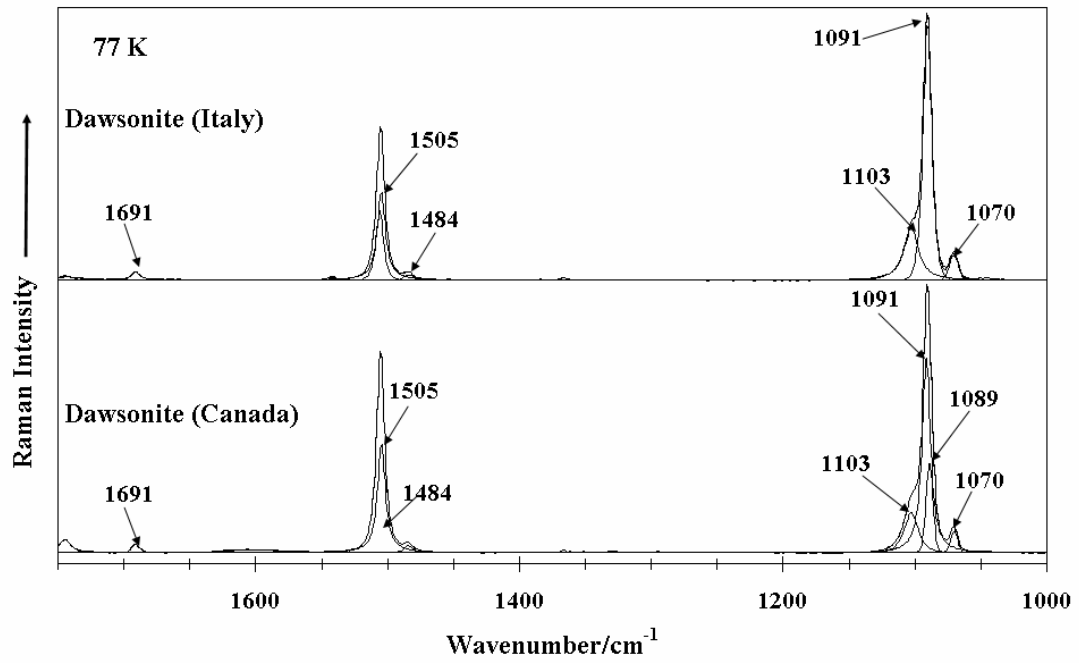


Figure 2b

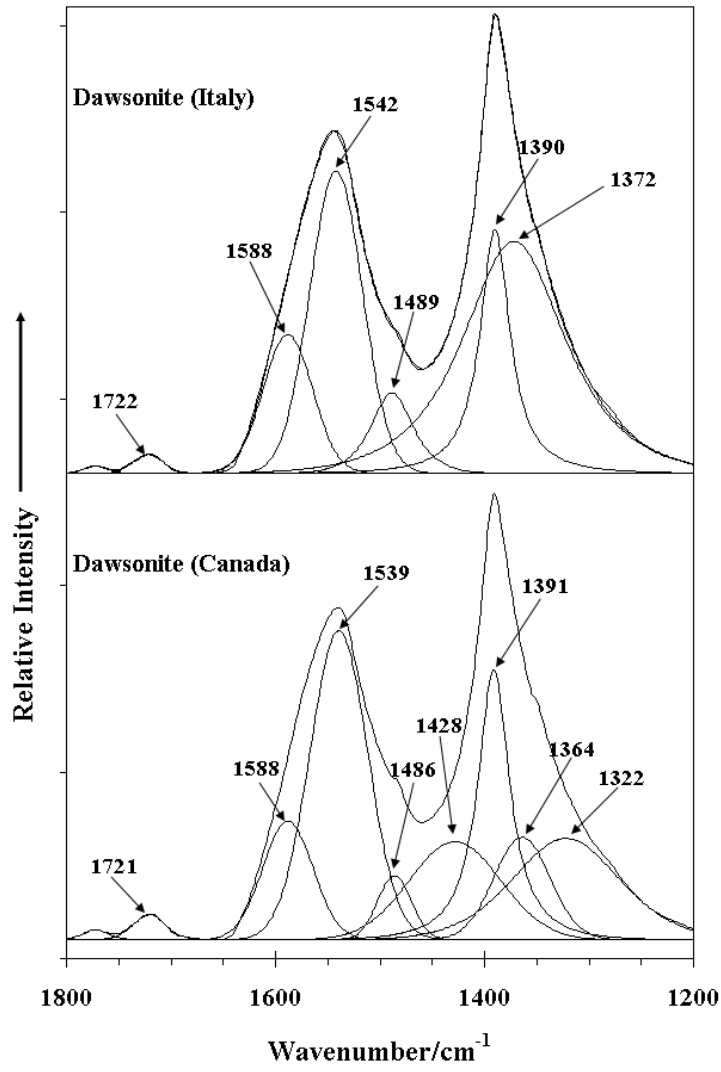


Figure 3

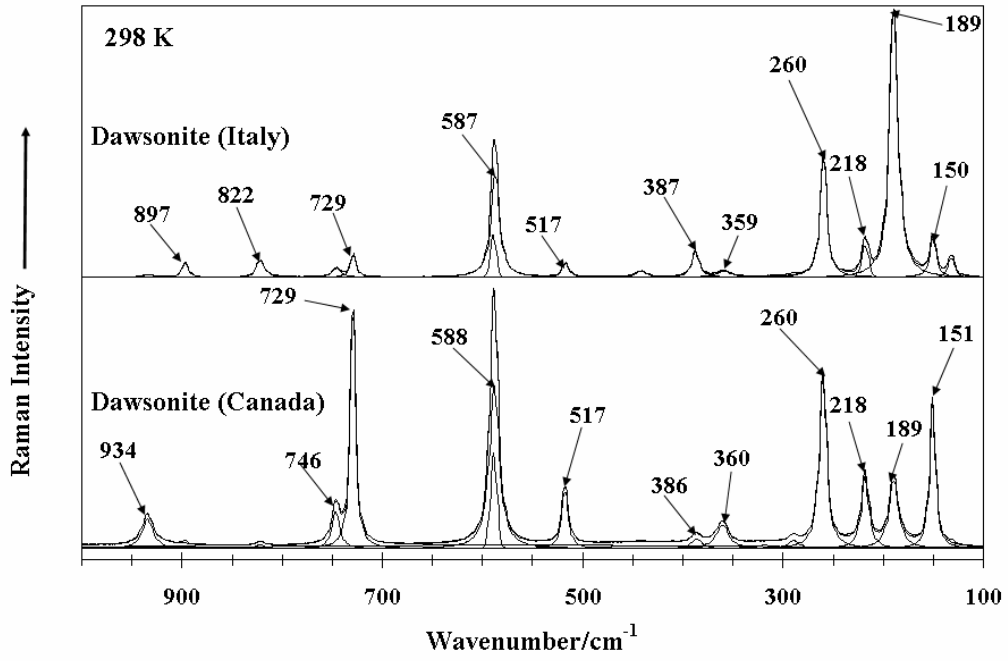


Figure 4a

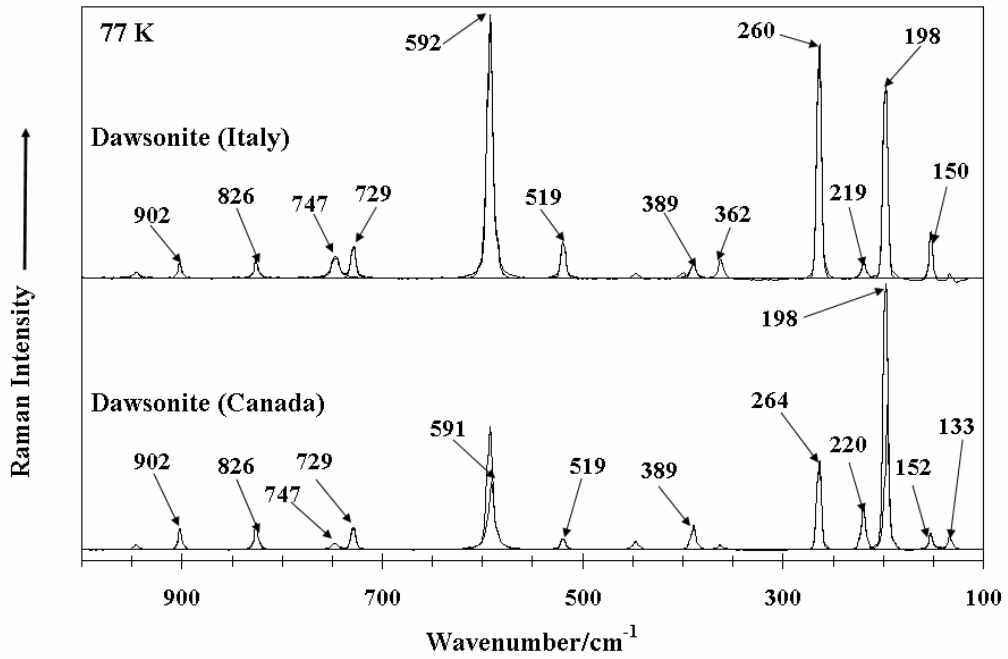


Figure 4b

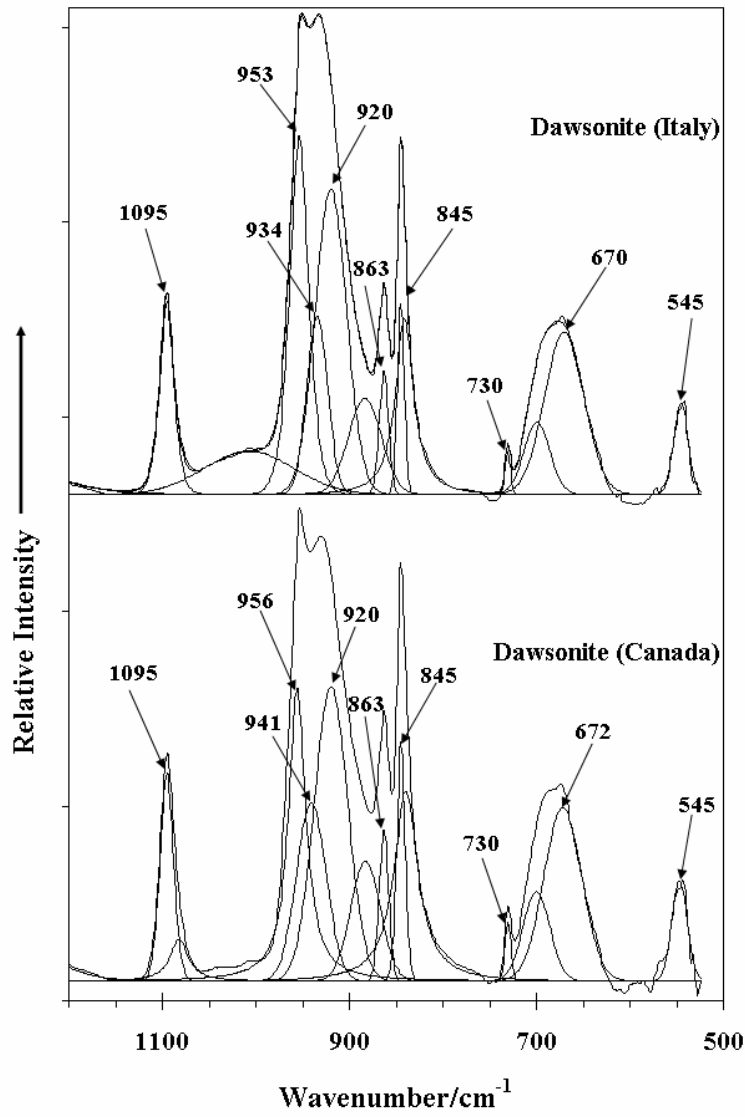


Figure 5

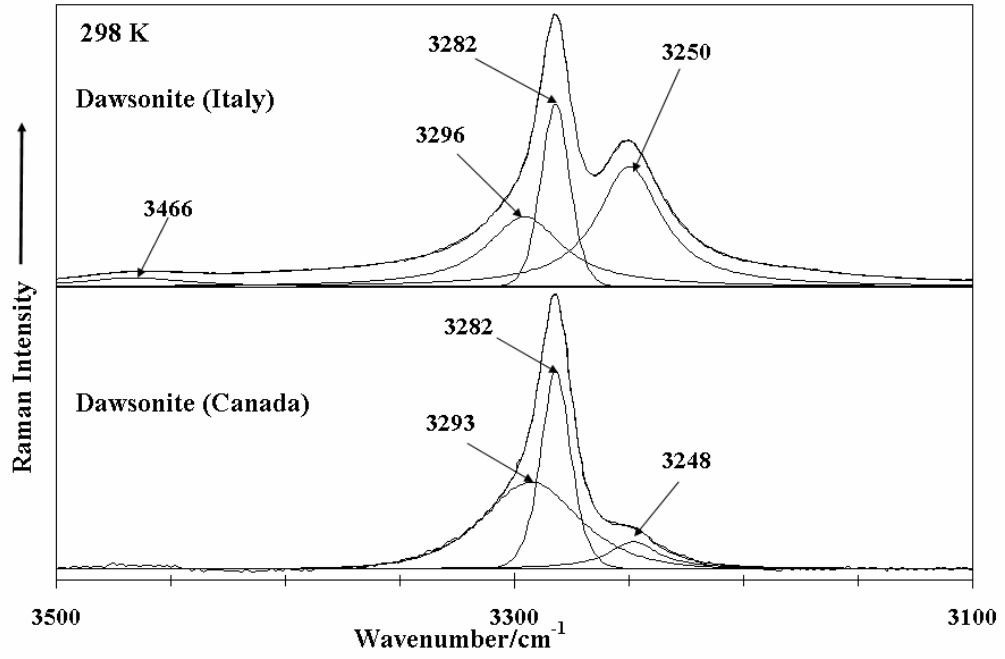


Figure 6a

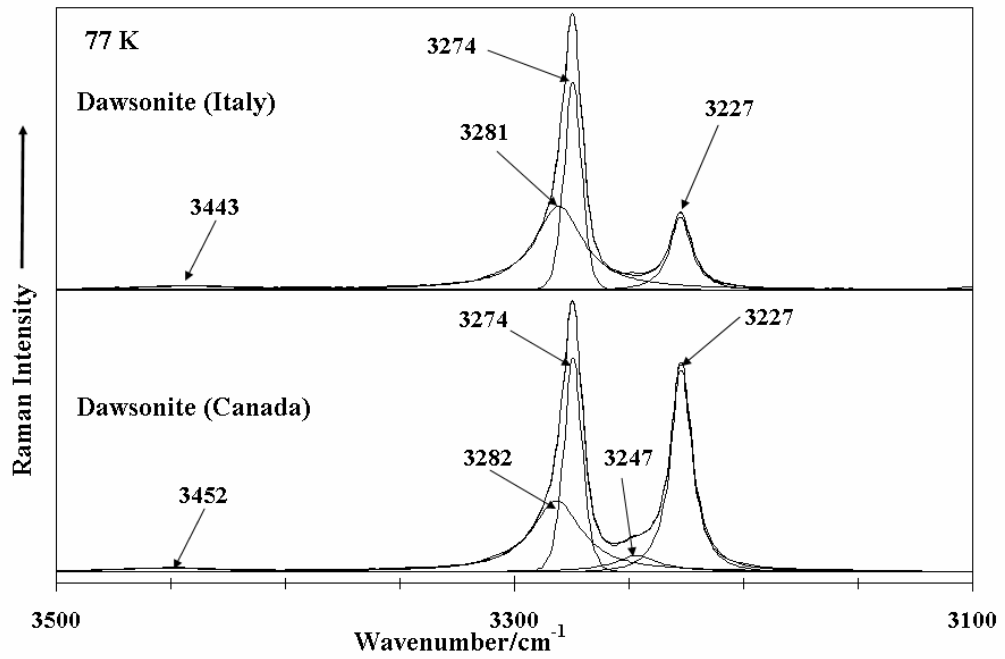
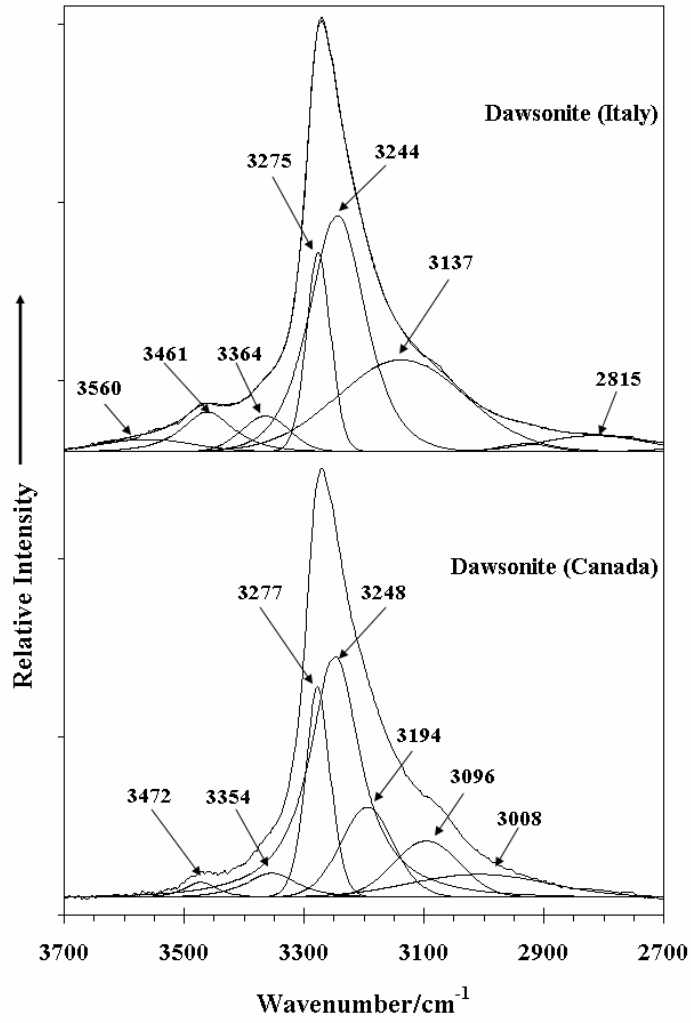


Figure 6b





**Figure 7**